University of Reading

Robustness of serial clustering of extratropical cyclones to the choice of tracking method

Article

Accepted Version

Pinto, J. G., Ulbrich, S., Economou, T., Stephenson, D. B., Karremann, M. K. and Shaffrey, L. C. ORCID: https://orcid.org/0000-0003-2696-752X (2016) Robustness of serial clustering of extratropical cyclones to the choice of tracking method. Tellus A, 68. 32204. ISSN 1600-0870 doi: 10.3402/tellusa.v68.32204 Available at https://centaur.reading.ac.uk/66165/

It is advisable to refer to the publisher's version if you intend to cite from the work. See Guidance on citing.

To link to this article DOI: http://dx.doi.org/10.3402/tellusa.v68.32204

Publisher: Co-Action Publishing

All outputs in CentAUR are protected by Intellectual Property Rights law, including copyright law. Copyright and IPR is retained by the creators or other copyright holders. Terms and conditions for use of this material are defined in the End User Agreement.

www.reading.ac.uk/centaur

University of Reading

CentAUR

Central Archive at the University of Reading

Reading's research outputs online

Robustness of serial clustering of extra-tropical cyclones to the choice of tracking method

Joaquim G. Pinto*
Department of Meteorology, University of Reading, UK and
Institute for Geophysics and Meteorology, University of Cologne, Germany

Sven Ulbrich
Institute for Geophysics and Meteorology, University of Cologne, Germany

Theodoros Economou, David B. Stephenson,

Department of Mathematics, University of Exeter, UK

Melanie K. Karremann
Karlsruhe Institute of Technology, Institute of Meteorology and Climate Research, Germany

Len C. Shaffrey
NCAS-Climate, Department of Meteorology, University of Reading, UK

Tellus A - Thematic Cluster

"Intercomparison of Mid-Latitude Storm Diagnostics"

Accepted version 4 July 2016

doi:10.3402/tellusa.v68.32204

*Corresponding author address: Joaquim G. Pinto, Department of Meteorology, University of Reading, Earley Gate, PO Box 243, Reading RG6 6BB, United Kingdom
E-mail: j.g.pinto@reading.ac.uk

Abstract

Cyclone clusters are a frequent synoptic feature in the Euro-Atlantic area. Recent studies have shown that serial clustering of cyclones generally occurs on both flanks and downstream regions of the North Atlantic storm track, while cyclones tend to occur more regulary on the eastern side of the North Atlantic basin near Newfoundland. This study explores the sensitivity of serial clustering to the choice of cyclone tracking method using cyclone track data from 15 methods derived from ERA-Interim data (1979-2010). Clustering is estimated by the dispersion (ratio of variance to mean) of winter (DJF) cyclones passages near each grid point over the Euro-Atlantic area. The mean number of cyclone counts and their variance are compared between methods, revealing considerable differences, particularly for the latter. Results show that all different tracking methods qualitatively capture similar large-scale spatial patterns of underdispersion / overdispersion over the study region. The quantitative differences can primarily be attributed to the differences in the variance of cyclone counts between the methods. Nevertheless, overdispersion is statistically significant for almost all methods over parts of the Eastern North Atlantic and Western Europe, and is therefore considered as a robust feature. The influence of the North Atlantic Oscillation on cyclone clustering displays a similar pattern for all tracking methods, with one maximum near Iceland and another between the Azores and Iberia. The differences in variance between methods are not related with different sensitivities to the NAO, which can account to over 50% of the clustering in some regions. We conclude that the general features of underdispersion / overdispersion of extra-tropical cyclones over the North Atlantic and Western Europe is robust to the choice of tracking method. The same is true for the influence of the North Atlantic Oscillation on cyclone dispersion.

Keywords: Poisson process; extra-tropical cyclones, clustering, dispersion statistics, North Atlantic, Europe, IMILAST, reanalysis.

1. Introduction

Extra-tropical cyclones over the North Atlantic play a key role in determining the weather and climate of Western Europe. Cyclones have a tendency to serially cluster close to Europe (Mailer et al., 2006), particularly extreme ones (Vitolo et al., 2009; Pinto et al., 2013), which can lead to severe socio-economic impacts and cumulative losses. A recent example is the unusually large number of storms that affected the British Isles during the winter of 2013/2014 (Matthews et al., 2014). The winter of 2013/2014 was characterized by exceptionally wet and windy conditions in this region, and the resulting wind damage and widespread coastal and inland flooding had a considerable impact on infrastructure and transportation (Huntingford et al., 2014). Such stormy winters are characterized by the frequent occurrence of cyclone families (Bjerknes and Solberg, 1922).

Pinto et al. (2014) recently provided evidence that the occurrence of cyclone clusters is governed by a persistent, zonally orientated and extended eddy-driven polar jet stream over the Eastern North Atlantic and Western Europe, which drives the North Atlantic cyclones towards the British Isles and sometimes further into Central Europe. The maintenance of these large-scale conditions is supported by two-sided Rossby wave breaking over the North Atlantic (Hanley and Caballero, 2012; Gómara et al, 2014; Messori and Caballero, 2015). Pinto et al. (2014) demonstrated for four selected stormy periods 1990, 1993, 1999 and 2007, that secondary cyclogenesis (new storms develop on the trailing fronts of previous storms, cf. Parker, 1998) further contributes to the occurrence of cyclones clusters arriving into Western Europe in rapid succession.

If cyclone occurrences at a certain area were completely random, then they can be statistically modelled as Poisson (point) process. Deviations from a Poisson process can indicate whether cyclones occur either in a more clustered (cyclones occur in groups) or a more regular way (time between occurrences almost constant). Thus, implementing Poisson models to cyclone

count data can be used as a way of quantifying the amount of clustering/regularity (e.g., Mailier et al., 2006; Vitolo et al., 2009; Pinto et al., 2013; Blender et al., 2015; Economou et al., 2015). The common result from these publications is that cyclone clustering (overdispersion) occurs on both flanks and downstream of the North Atlantic storm track (Mailier et al., 2006, their Fig. 6), while regularity (underdispersion) is found near the core of the storm track by Newfoundland. This pattern is a robust feature in different reanalysis datasets (Pinto et al., 2013, their Fig. 3). Global circulation models also broadly capture this spatial pattern of overdispersion / underdispersion over the North Atlantic and Western Europe (Economou et al., 2015, their Fig. 2).

Previous studies (Mailier et al., 2006; Vitolo et al., 2009) have shown that large-scale atmospheric modes of variability such as the North Atlantic Oscillation (NAO, e.g. Hurrell et al., 2003) have a strong influence on cyclone clustering. The NAO is the dominant large-scale atmospheric pattern over the North Atlantic and Western Europe. The NAO has two centers of action, the Azores high and the Icelandic low, and its index is a proxy for the strength of the westerlies over the Northeast Atlantic. Thus, the NAO largely determines the weather conditions over this area, particularly in wintertime. The NAO varies on time scales ranging from days to centuries, but with dominant interdecadal to decadal time scales (Pinto and Raible, 2012). Cyclone tracks are shifted northward and extended downstream in positive NAO phases, while they are shorter and shifted southward in negative NAO phases (e.g., Pinto et al., 2009). Furthermore, the NAO and other large-scale modes affect both the frequency and intensity of extratropical cyclones over the North Atlantic (Hunter et al., 2016). The existence of clustering has been associated with NAO variability (e.g. Mailier et al., 2006), as a prolonged time period with a dominant NAO phase will tend to direct cyclones over the North Atlantic towards a specific area (Pinto et al., 2009), thus enhancing (reducing) the number of cyclone counts in that specific area (other areas). Simple models have been

98 developed to analyse the relationship between NAO and cyclone activity, revealing that a
99 considerable part of the clustering is related to NAO variability (e.g. Mailier et al., 2006;
100 Vitolo et al., 2009; Economou et al., 2015). This is true for both reanalysis datasets and global
101 climate models.
102 Publications quantifying cyclone clustering over the North Atlantic have used single cyclone
103 tracking methods, either Hodges (1994), Murray and Simmonds (1991) or Blender et al.
104 (1997). As noted by Neu (2013), there is no single scientific definition of what an extratropical
105 cyclone is, and thus no consensus on the best atmospheric variable to use, leading to different
106 approaches for identifying and tracking cyclones. As a consequence, cyclone statistics and
107 characteristics differ depending on the cyclone tracking method and/or the key variable used
108 (e.g., Hoskins and Hodges, 2002; Raible et al., 2008; Rudeva et al., 2014). One of the
109 objectives of the Intercomparison of Mid-Latitude Storm Diagnostics (IMILAST) project is to
110 understand which cyclone statistics are robust to the choice of tracking algorithm (Neu et al.,
111 2013). Such an assessment is necessary to be able to provide objective information to
112 stakeholders regarding cyclone activity in general and windstorms in particular (Hewson and
113 Neu, 2015).
114 The present manuscript is a contribution to the IMILAST project. The main question explored
115 in this study is how robust the general features of underdispersion / overdispersion over the
116 study area are to the choice of cyclone tracking method. With this aim, we perform for the first
117 time a multi-tracking approach analysis of clustering over the North Atlantic and Europe. The
118 second aim is to evaluate how the NAO influence on cyclone clustering depends on the choice
119 of tracking method. Section 2 describes the datasets and methodologies used. The
120 quantification of cyclone passages is explained in section 3, together with a description of
121 mean and variance of counts. Section 4 presents the clustering as identified for all the 15

122 methods and investigates spread between methods. Section 5 quantifies the links between
123 clustering and the NAO variability. A short conclusion follows.
124
125 **2. Data and Methods**
126 *The IMILAST project cyclone track dataset*
127 One of the main objectives of the IMILAST project is to document and understand the
128 sensitivity of the representation of cyclone activity and extreme windstorms in reanalysis
129 datasets and global climate model simulations to the choice of cyclones tracking method. In
130 particular, the IMILAST team has been evaluating which cyclone features are largely
131 independent of the tracking method used (and hence can be regarded as robust), and which
132 features differ between tracking methods. In a first analysis, Neu et al. (2013) concluded that
133 differences between methods are typically small for long-lived, transient, deep, intense lows
134 over large oceanic basins. This is not unexpected, as extremes associated with extratropical
135 cyclones (e.g., minimum sea level pressure, vorticity, peak winds) are strongly inter-related
136 (Economou et al., 2014). On the other hand, considerable discrepancies between tracking
137 methods are found for short-lived, shallow, and slow moving systems, particularly over areas
138 like the Mediterranean or over the continents (Neu et al., 2013; Lionello et al., 2016). More
139 details on the inter-comparison strategy, general results and proposed future directions of
140 research are discussed in Hewson and Neu (2015).
141 The cyclone track database from the IMILAST project is used here to estimate the dispersion
142 of cyclone counts over the North Atlantic and Europe. The cyclone tracks were derived with
143 multiple cyclone tracking methods (see Neu et al., their Table 1) based on European Centre for
144 Medium-Range Weather Forecasts (ECMWF) Interim Reanalysis (ERA-Interim; Dee et al.,
145 2011). The horizontal resolution of the dataset is T255 (approximately 0.75°x0.75° latitude /
146 longitude), with 60 vertical levels from surface up to 0.1 hPa. The data was interpolated to

147 1.5°x1.5° and made available to all IMILAST participants. The investigation period is
148 December 1979 to February 2010 (at 6-hourly resolution), and only winter months are
149 analysed (December, January, February: DJF). Here, we consider results from 14 tracking
150 methods from the IMILAST project (cf. Table 1, M02-M22). Additionally, we considered also
151 cyclone tracks derived with the Hodges tracking method (Hodges, 1994, 1999; Hodges et al.,
152 2011, HOD) for the same time period and set up as the IMILAST tracking data. Tracks over
153 high orography (>1500 m) are not considered (e.g. Greenland, Atlas Mountains) and such
154 areas are disregarded in this study. All tracks have a lifetime of at least 24 hours (five time
155 frames). For specific details on the individual methods see references inserted in Table 1.
156 Comparisons between the tracking methods are presented in e.g., Raible et al. (2008), Neu et
157 al. (2013), Rudeva et al. (2014) and Lionello et al. (2016). Several case studies are discussed
158 in Hewson and Neu (2015), including comparisons to observations. The colors of the method
159 in Figures 1 and 5 correspond to the type of method (cf. Table 1): Green colours for 850 hPa
160 vorticity (M07, M18, M21, HOD), grey for 850 hPa geopotential height minimum contour
161 (M14), orange/brown for mean sea level (MSLP) minimum (M12, M15, M16, M20), red for
162 MSLP gradient or minimum contour (M06, M08, M22), and blue for Laplacian of MSLP
163 (M02, M09, M10).
164
165 *Quantification of clustering*
166 The occurrence of random events in time can be represented by the homogeneous Poisson
167 process (Cox and Isham, 1980). If the events (cyclones) arise with a rate of occurrence λ, then
168 the number of events y in a time interval T is Poisson distributed (random), with mean ($\bar{y}$) and
169 sample variance (s_y^2) both equal to λT, and thus $s_y^2 / \bar{y} = 1$. Deviations from the Poisson
170 process indicate a non-random arrival of cyclones over time, in the sense that events
171 systematically occur in a more clustered (in groups) or a more regular way (equal spacing in

time; cf. Fig. S1). These deviations from the Poisson process can be used to assess the degree of clustering, and following Mailier et al. (2006), we use the dispersion statistic:

$$\phi = \frac{{s_y}^2}{\bar{y}} - 1. \quad (1)$$

A Poisson process (${s_y}^2 = \bar{y}$) with a constant rate of occurrence λ implies $\phi = 0$. Positive values of ϕ indicate clustering (overdispersion; ${s_y}^2 > \bar{y}$), and negative values of ϕ indicate regularity (underdispersion; ${s_y}^2 < \bar{y}$; cf. Fig. S1). Following Pinto et al. (2013), events are defined as cyclone tracks intercepting a radius of influence around a certain grid point. An identification radius of 700 km was selected based on considerations related to cyclone sizes and potential impacts, so the rate is the number of cyclones that pass through this region with an area of $\pi \cdot 700\text{km}^2$ (see Pinto et al., 2013 for more details). When a cyclone track intercepts the circle for a selected grid point, the time corresponding to the nearest position to the circle center is counted (cf. Fig. 1a for an example). In this way, time series are obtained for each method (Fig. 1b). This approach is applied at each location (grid point) and was recently used to estimate clustering of cyclones simulated by CMIP5 global climate models (Economou et al., 2015). For each winter (DJF), cyclone counts (y_i) are computed for the period 1979/80-2009/10 to produce a time-series of counts $\{y_1, y_2, \ldots, y_n\}$ at each grid point, where *n* is the number of winters.

Relationship with the North Atlantic Oscillation

As explained in Economou et al. (2015), overdispersion can be approximated by

$$\phi' = 4\left(s_{\sqrt{y}}\right)^2\text{-1}. \quad (2)$$

where $\left(s_{\sqrt{y}}\right)^2$ is the sample variance of $\sqrt{y}$, and thus

$$\left(s_{\sqrt{y}}\right)^2 = \frac{1}{n} \cdot \sum_{i=1}^{n} \left(\sqrt{y_i} - \overline{\sqrt{y}}\right)^2 = \bar{y} - \left(\overline{\sqrt{y}}\right)^2. \quad (3)$$

The square root transformation stabilizes the variance, i.e. removes the dependence between mean and variance. Economou et al. (2015) showed that this also allows a regression of $\sqrt{y}$ on the NAO, in order to quantify the possible influence of the NAO on dispersion:

$$\sqrt{y} = \alpha + \beta x + \varepsilon; \quad \varepsilon \sim N(0, \sigma^2) \quad (4)$$

where x is the seasonal mean of NAO. Parameters α and β are estimated from the data, and represent the intercept and slope parameters of the assumed linear relationship between $\sqrt{y}$ and the NAO. The term ε represents the error about the straight line, and is assumed to follow a Normal distribution with variance σ^2, which is also estimated from the data. To investigate whether the assumption that NAO is linearly related to $\sqrt{y}$ holds across all methods, we have additionally implemented an extended regression assuming a quadratic relationship:

$$\sqrt{y} = \alpha + \beta x + \gamma x^2 + \varepsilon; \quad \varepsilon \sim N(0, \sigma^2) \quad (5)$$

The estimated linear and quadratic relationships for two exemplary grid points near the Azores and Iceland are shown in Figures S2 and S3. In general, these plots indicate that there is no real difference between the linear and quadratic fits, so that the linear fit is retained. The NAO index is calculated following the methodology by Barnston and Livezey (1987), which is based on Rotated Principal Component Analysis. The monthly time series for December, January and February were provided by the Climate Prediction Center from the National Oceanic and Atmospheric Administration and averaged for each winter (DJF).

Using equation (4), it can be shown that

$$\phi' = 4\left(s_{\sqrt{y}}\right)^2 - 1 = 4\beta^2 (s_x)^2 + 4\sigma^2 - 1 \quad (6)$$

where $(s_x)^2$ is the sample variance of the NAO-index *x*. This allows to diagnose how much of the underdispersion can attributed to modulation of counts by NAO (the parameter β).

3. Quantification of cyclone passages on a grid point basis

Time series of cyclone counts for all 15 methods are first analysed at each grid point. As an example, we consider the grid point 55°N, 5°W centered over the British Isles and cyclone counts for January 2007 (Fig. 1), a period characterized by a large number of storms over this area (Pinto et al., 2014). The corresponding 700 km identification radius is shown in Fig. 1b. The cyclone passages within this area are indicated in the time line (Fig. 1a) and show some similarities but also differences for the individual methods: for example, the number of identified cyclones for this grid point and month ranges from 5 (M22) to 25 (M18). On the other hand, the main cyclones passing through this area (9, 10, 12, 13, 15, 18 and 20 January; cf. Pinto et al., 2014; their Figure 3) are captured by most methods. Fig. 1b shows the individual tracks for all methods for the cyclone passing on 13 January (named storm "Hanno" by the Free University of Berlin). The tracks show generally a good agreement for all methods in the main development phase, when all tracks are found within a corridor of a few 100 kilometers. Small differences between the tracks at this development stage are typical, given that the methods use different key variables for tracking: for example, the MLSP minima and 850 hPa vorticity maxima do not exactly overlap in an extra-tropical cyclone (e.g. Pinto et al., 2005; their Figure 1), with the vorticity maxima (e.g., M07, M18, HOD) typically being located south of the former (e.g. M02, M06). Less agreement is found at the beginning (different starting points) and particularly at the end of the cyclone tracks, which show diverging trajectories over Eastern Europe: while most methods show a zonal track towards southern Finland and further into Northern Russia, some of the vorticity methods (green) show

239 a track towards the Caspian Sea. Similar results have been found in previous case studies
240 analysed in the IMILAST project (Neu et al., 2013; their Figs 4 and 5).
241 Following this methodology, time series of cyclone counts are derived for each grid-point in
242 the domain 30°N – 70°N and 80°W – 20°E and for the whole study period (winters 1979/80 to
243 2009/10). The mean of counts $\bar{y}$ and their variance $(s_y)^2$, the two components needed to
244 estimate ϕ, are displayed in Figures 2 and 3 for all 15 cyclone tracking methods. The number
245 of tracks passing through a certain area ($\bar{y}$; Figure 2) is comparable to a cyclone track density
246 field, and depict higher magnitudes in areas with many transient cyclones. This is unlike
247 cyclone count statistics, in which cyclones can be counted multiple times in the same location
248 (cf. Pinto et al., 2005). Therefore, some intrinsic differences are found between Figure 2 and
249 Figure 1 from Neu et al. (2013), which shows cyclone count statistics. This reveals a larger
250 discrepancy between the algorithms compared to Neu et al. (2013), e.g. there is no common
251 peak south of Greenland for all methods (Figure 2).
252 Differences between tracking methods are identified both in terms of total numbers, position
253 of the North Atlantic storm track and regional aspects such as Mediterranean cyclones: For
254 example, methods M14, M21 and M22 show generally small cyclone numbers and relatively
255 weak activity over the Mediterranean Basin (Figure 2). This is not the case for other methods
256 such as M02, M06, M15 and M20. However, the general spatial pattern in mean counts over
257 the North Atlantic storm track qualitatively agrees between methods. Some of the spatial
258 differences between methods can be explained by the choice of variable used in the tracking.
259 For example, cyclone tracks based on 850 hPa vorticity (VORT) are typically displaced
260 southwards to cyclone tracks derived from MSLP pressure minimum (cp. M15 and M18).
261 Systematic discrepancies between the various cyclone track algorithms also play a role for the
262 identified differences. See also Neu et al. (2013) for more details. Specific differences within

263 the Mediterranean Basin are discussed in Lionello et al. (2016) and will not be further
264 analysed here.
265 The variance of counts $(s_y)^2$ shows more diverse results (Figure 3). Spatial patterns typically
266 display a maximum of activity south of Greenland, which often extends towards Northern
267 Europe. However, the relative maximum over Western / Central Europe is not found for some
268 methods (e.g. M16, M21), or is displaced in others (M06, M18) to around 50°N–55°N over
269 the Eastern North Atlantic. While this relative maximum is also found for other methods (e.g.
270 M02, M15) it is not the dominant feature. In terms of numbers, the differences in $(s_y)^2$
271 between methods are even larger than for $\bar{y}$, with values differing by an order of magnitude in
272 some areas, e.g. south of Greenland.
273
274 **4. Quantification of clustering**
275 The estimates of ϕ for the different methods are shown in Figure 4. The general spatial pattern
276 qualitatively agrees between tracking methods, e.g. an area of ϕ<0 identified over the western
277 North Atlantic (regularity or underdispersion; blue colours), while ϕ>0 (clustering or
278 overdispersion; red colours) is found on northern and southern flanks and the downstream
279 region of the North Atlantic storm track (cp. Mailier et al., 2006; Pinto et al., 2013).
280 Considering the whole study area, overdispersion (red) tends to dominate for some methods
281 (e.g., M15, M20), while underdispersion (blue) dominates for others (e.g., M21, M22).
282 However, most methods show a balance between the two features (e.g. M02, M06, M18), in
283 line with previous works (Mailier et al., 2006; Pinto et al., 2013). While all methods show
284 overdispersion over Western Europe, the magnitude of ϕ clearly differs between methods. For
285 the example grid point 55°N, 5°W, ϕ is positive for all methods (clustering), but ranges from
286 0.27 (M21) to 4.73 (M20). Differences appear to be dominated primarily by the variance of
287 winter counts (cf. Figure 3).

To provide further insight into the differences between methods, we analyse in detail the relations between $\bar{y}$ and $(s_y)^2$ for 55°N, 5°W. In Figure 5, the mean is plotted against the variance, and the lines corresponding to ϕ =0, 1, 2, 3, 4, and 5 are shown for orientation. Half of the methods are found in the range between ϕ =0.86 and 1.32, and four methods around 2.0 (M07, M08, M09, M14). Methods M15, M20 and M21 are outliers: the two former methods (both based on MSLP) display a much higher $(s_y)^2$ compared to $\bar{y}$, while for the latter $(s_y)^2$ and $\bar{y}$ are small and roughly equal. The statistical significance bounds for the Poisson distribution (ϕ =0) is estimated using parametric bootstrapping: 10000 time series of 30 counts are generated for each mean value (1-55) assuming a Poisson distribution. For each mean value, the empirical 95% quantile of those 10000 variance values is used to construct a 95% confidence interval (gray area around ϕ =0 in Figure 5). This implies that dispersion values for all but two methods (M21, HOD) significantly deviate from Poisson. Similar results are found for other grid points over the Eastern North Atlantic and Western Europe (not shown), revealing the robustness of overdispersion of cyclone counts for this area.

The range of the horizontal axis (in Figure 5), which shows the mean, is much smaller than the range of the vertical axis, which shows the variance. This indicates that differences in $(s_y)^2$ are the primary driver behind the differences in ϕ. For example, $\bar{y}$ is actually quite similar for M20 and M21 (20.9 and 18.5, respectively), while $(s_y)^2$ and thus ϕ are very different. On the other hand, the consistency of results between M02 and M10 is noteworthy: these approaches basically use the same tracking method with different parameters, and provide very similar values of ϕ (1.21 and 1.32) despite the differences in $\bar{y}$. Methods displaying underdispersion over most of the study area (e.g., M21, M22) typically have a small number of cyclone counts (cf. Fig. 2), but the dominant factor for the differences in ϕ remains $(s_y)^2$. It is noteworthy that the two methods with the highest ϕ values (M15, M20) are MSLP minimum methods

312 (orange/brown). However, other MSLP minimum methods (M12, M16) show values closer to
313 the other approaches. It is therefore difficult to associate the diversity of ϕ results with
314 particular features of tracking methods. This result is consistent with the conclusions of Neu et
315 al. (2013) and Rudeva et al. (2014) regarding cyclone characteristics and their possible
316 dependence on the tracking method.
317
318 **5. Relationship with the NAO**
319 The recent study by Economou et al. (2015) showed that a considerable part of the
320 overdispersion identified based on ERA-Interim reanalysis cyclone tracks derived with the
321 HOD approach is due to the modulation of cyclone counts by the NAO. In order to investigate
322 the NAO influence on cyclone clustering, dispersion is now quantified following Economou et
323 al. (2015), where ϕ is approximated by $\phi' = 4\left(s_{\sqrt{y}}\right)^2$-1 (equation 2). Results are shown in
324 Figure 6 for each tracking method. The two estimation methods for ϕ are very similar (cp.
325 Figs 4 and 6), implying that the ϕ' is a good approximation to ϕ. In the following, we use this
326 approximation to estimate the contribution of the NAO index to the dispersion index
327 according to equation (6).
328 The linear relationship between the strength of the NAO x and $\sqrt{y}$ is quantified by the
329 parameter β. The result is a dipolar structure, revealing a positive pole near Iceland and a
330 negative pole over the Azores (cf. Figure 7). This systematic influence of the NAO-Phase on
331 clustering can now be quantified as $4\beta^2(s_x)^2$ (equation 6). Figure 8 shows the NAO
332 contribution for each method, revealing two maxima, one north and one south of the North
333 Atlantic storm track. This general spatial pattern is in good agreement with Economou et al.
334 (2015) who considered cyclone tracks derived with HOD method and ERA-40 data (Uppala et
335 al., 2005). The North Atlantic storm track moves latitudinally depending on the NAO-phase,
336 leading to the two maxima of NAO influence on clustering on the flanks of the storm track.

However, there are differences in the detail between the 15 methods, both in terms of spatial pattern and magnitude. This can be partly explained by the relationship between the NAO influence on dispersion and the magnitude of dispersion itself per method (compare Figures 4 and 8). For example, a strong influence of the NAO on the clustering of cyclones is found in regions and methods where overdispersion is high (cp. Figure 4 and Figure 8 for M07, M08, M15, M20 near the Alps). The spatial pattern of NAO influence also shows some differences over Europe: for example, while the region with low NAO influence (white) is located over Northern Europe for most methods, a few methods have this region over Central Europe (M10, M18) or over France (M20). The spatial variability of the NAO-influence is high for some methods (M07, M08, M15), which indicates a larger uncertainty of the β estimate. In general, it is difficult to associate the different types of methods (e.g. using vorticity or MSLP as the cyclone tracking variable) with a specific type of behavior regarding the NAO influence on cyclone clustering over the North Atlantic and Europe, but the general agreement between the methods is encouraging.

The large differences in the number of counts between the methods leads to strong differences in β and therefore also on the absolute contribution of the NAO to overdispersion. As all the effects contributing to clustering can be quantified as $4\beta^2(s_x)^2 + 4\sigma^2$ (equation 6), the relative contribution of the NAO is defined as $4\beta^2(s_x)^2/(4\beta^2(s_x)^2 + 4\sigma^2)$ and shown in Figure 9. A similar pattern to Figure 8 is revealed, with the two maxima near Iceland and the Azores, plus additional maxima over Central Europe or near Newfoundland. The relative contribution of the NAO to clustering exceeds 50% for some methods, particularly south of Iceland and in the region between Azores and Iberia. The intensity and extension of the area around each of the two maxima differ. For example, for M02, both maxima are approximately equally strong, while for M18 the southern maximum is more pronounced. This suggests a stronger (weaker) contribution of other processes than the NAO to the clustering for one

362 (other) maximum. Comparing the figures 3 and 9, it is quite apparent that there is no clear link
363 between the difference in variance between methods and the sensitivity to the NAO.
364
365 **6. Conclusions**
366 The main objective of this paper was to assess if the cyclone clustering over the eastern North
367 Atlantic and Europe is a robust feature using results from 15 cyclone tracking methods. A
368 second objective was to evaluate whether the relationship between NAO and clustering
369 depends on the choice of the tracking method. The main findings of this study are as follows:
370
371 • The general spatial pattern of the cyclone dispersion statistic (ϕ), as previously
372 identified with single tracking methods, is qualitatively captured by all methods:
373 underdispersion (regularity) is identified near the core of the North Atlantic storm
374 track near Newfoundland, while overdispersion (clustering) can be found over the
375 eastern North Atlantic and Western Europe, particularly on both sides and downstream
376 of the North Atlantic storm track.
377 • Quantitative differences in the values of ϕ are identified between methods. Some
378 methods display predominantely underdispersion (regularity) over the study area,
379 while others indicate overdispersion (clustering) over almost the whole study area.
380 • The differences in ϕ can be primarily attributed to the differences in the variance of
381 cyclone counts between the methods.
382 • Significant overdispersion is identified for almost all methods over parts of the Eastern
383 North Atlantic and Western Europe, indicating the robustness of cyclone clustering in
384 this area. Still, the magnitude of ϕ may vary strongly between methods.
385 • The statistical link between NAO and clustering of cyclone tracks found for all
386 methods and is thus a robust feature: in accordance with previous studies, maxima on

387 both sides of the main storm track are identified, though with slightly different
388 magnitudes and spatial extension.
389 • The explained variance of the NAO on clustering exceeds 50% for some tracking
390 methods and locations. The differences in the variance of cyclone counts cannot be
391 attributed to different sensitivities to the NAO.
392
393 We conclude that both the general pattern of underdispersion / overdispersion over the North
394 Atlantic and Western Europe and the dipolar pattern of NAO influence on dispersion are
395 largely independent from the choice of tracking method and hence from the definition of a
396 cyclone. In particular, overdispersion of cyclone counts is identified for all methods over the
397 Western Europe, and can therefore be considered as a robust feature. This is important and
398 valuable information for stakeholders, such as the insurance industry, for whom the clustering
399 of extreme cyclones is a major economic risk.
400 The present results suggest that estimates of cyclone clustering obtained with single tracking
401 methods can be regarded as qualitatively representative for a wider range of tracking methods.
402 This is particularly important because cyclone clustering may change under future climate
403 conditions (Pinto et al., 2013). Given the large sampling uncertainty, such potential changes
404 may not be detectable in single 30-year climate model simulations (Economou et al., 2015).
405 Still, Karremann et al. (2014) has recently provided evidence based on a large ensemble of
406 simulations with a single global circulation model that cumulative annual losses associated
407 with extra-tropical cyclones may increase over most of Europe in future decades due to a
408 combination of changes in potential loss magnitude and changes in storm clustering.
409 Future research could analyse differences between tracking methods also in higher resolution
410 reanalysis datasets such as NASA-MERRA (Rienecker et al., 2011). The higher spatial and
411 temporal resolution will permit a better quantification of the features identified here and a

more detailed dynamical analysis similar to Pinto et al. (2014). Another interesting line of research is to quantify the role of the jet location and intensity for cyclone clustering across Western Europe. Preliminary results (for the grid point 55°N, 5°W) indicate that winters with a stronger jet also have a higher number of counts for all methods, particularly when the jet is located around 45°N-50°N (not shown). Finally, it will be interesting to investigate clustering of extratropical cyclones in global circulation models in more detail, taking into account how cyclones and cyclone clustering are represented at different resolutions, evaluating the representation of the associated physical processes, and analysing how results depend on the tracking method.

Acknowledgements

The authors would like to thank Swiss Re for sponsoring the Intercomparison of Mid-Latitude Storm Diagnostics (IMILAST) project. T.E. and D.B.S. were supported by NERC project CREDIBLE. We thank the European Center of Medium Range Weather Forecast (ECMWF, www.ecmwf.int) for the ERA-Interim reanalysis, and the Climate Prediction Center from the National Oceanic and Atmospheric Administration for the NAO index (http://www.cpc.ncep.noaa.gov/products/precip/CWlink/pna/nao.shtml). We thank all the members of the IMILAST project (www.proclim.ch/imilast) for making the cyclone tracks available. We also thank Kevin Hodges for making the cyclone tracks available for this study and for discussions. The present manuscript profited from discussion with various members of the IMILAST project group. We are thankful to the two anonymous reviewers for their valuable comments and suggestions on a previous version of this manuscript.

References

Akperov, M. G., Bardin, M. Y., Volodin, E. M., Golitsyn, G. S. and Mokhov, I. I. 2007. Probability distributions for cyclones and anticyclones from the NCEP/NCAR reanalysis data and the INM RAS climate model. *Izvest. Atmos. Ocean. Phys.* **43**, 705-712. doi: 10.1134/S0001433807060047.

Bardin, M. Y. and Polonsky, A. B. 2005. North Atlantic Oscillation and synoptic variability in the European-Atlantic region in winter. *Izvest. Atmos. Ocean. Phys.* **41**, 127-136.

Barnston, A. G., and Livezey, R. E. 1987. Classification, seasonality and persistence of low-frequency atmospheric circulation patterns. *Mon. Weather Rev.* **115**, 1083–1126. doi: 10.1175/1520-0493(1987)115<1083:CSAPOL>2.0.CO;2.

Blender, R., Fraedrich, K., and Lunkeit, F. 1997. Identification of cyclone track regimes in the North Atlantic. *Q. J. Roy. Meteorol. Soc.* **123**, 727-741. doi: 10.1002/qj.49712353910.

Blender R., Raible, C.C., and Lunkeit, F. 2015. Non-exponential return time distributions for vorticity extremes explained by fractional Poisson processes. *Q. J. Roy. Meteorol. Soc.* **141**, 249–257. doi: 10.1002/qj.2354.

Bjerknes, J., and Solberg, H. 1922. Life cycle of cyclones and the polar front theory of atmospheric circulation, *Geofys. Publ.* **3**, 3–18.

Cox, D. R., and Isham, V. 1980. Point Processes, pp. 188, Chapman and Hall/CRC, London.

Dee, D. P., Uppala, S. M., Simmons, A. J., Berrisford, P., Poli, P., and co-authors. 2011. The ERA-Interim reanalysis: Configuration and performance of the data assimilation system. *Q. J. Roy. Meteorol. Soc.* **137**, 553–597. doi: 10.1002/qj.828.

Economou, T., Stephenson, D. B., Ferro, C. A. T. 2014. Spatio-temporal modelling of extreme storms. *Ann. Appl. Stat.* **8**, 2223-2246. doi:10.1214/14-AOAS766.

458 Economou, T., Stephenson, D. B., Pinto, J. G., Shaffrey, L. C., Zappa, G. 2015. Serial
459 clustering of extratropical cyclones in historical and future CMIP5 model simulations. *Q. J.*
460 *Roy. Meteorol. Soc.* **141**, 3076–3087. doi: 10.1002/qj.2591.
461 Flaounas, E., Kotroni, V., Lagouvardos, K. and Flaounas, I. 2014. CycloTRACK (v1.0):
462 Tracking winter extratropical cyclones based on relative vorticity: Sensitivity to data
463 filtering and other relevant parameters. *Geosci. Model Dev.* **7**, 1841-1853. doi:
464 10.5194/gmd-7-1841-2014.
465 Gómara, I., Pinto, J. G., Woollings, T., Masato, G., Zurita-Gotor, P. and Rodríguez-Fonseca,
466 B. 2014. Rossby wave-breaking analysis of explosive cyclones in the Euro-Atlantic sector,
467 *Q. J. Roy. Meteorol. Soc.* **140**, 738–753. doi: 10.1002/qj.2190.
468 Hanley, J., and Caballero, R. 2012. The role of large-scale atmospheric flow and Rossby wave
469 breaking in the evolution of extreme windstorms over Europe. *Geophys. Res. Lett.* **39**,
470 L21708. doi: 10.1029/2012GL053408.
471 Hewson, T. D. 1997. Objective identification of frontal wave cyclones. *Meteorol. Appl.* **4**,
472 311-315. doi: 10.1017/S135048279700073X.
473 Hewson, T. D. and Titley, H. A. 2010. Objective identification, typing and tracking of the
474 complete lifecycles of cyclonic features at high spatial resolution. *Meteorol. Appl.* **17**, 355-
475 381. doi: 10.1002/met.204.
476 Hewson, T. D. and Neu, U. 2015. Cyclones, windstorms and the IMILAST project. *Tellus A*
477 **67**, 27128, doi: 10.3402/tellusa.v67.27128
478 Hodges, K. I. 1994. A general method for tracking analysis and its application to
479 meteorological data. *Mon. Weather Rev.* **122**, 2573–2585. doi: 10.1175/1520-
480 0493(1994)122<2573:AGMFTA>2.0.CO;2.
481 Hodges, K. I. 1999. Adaptive constraints for feature tracking. *Mon. Weather Rev.* **127**, 1362–
482 1373. doi: 10.1175/1520-0493(1999)127<1362:ACFFT>2.0.CO;2.

Hodges, K. I., Lee, R. W., and Bengtsson, L. 2011. A comparison of extratropical cyclones in recent reanalyses ERA-Interim, NASA MERRA, NCEP CFSR, and JRA-25. *J. Clim.* **24**, 4888–4906. doi: 10.1175/2011JCLI4097.1.

Hoskins, B. J. and Hodges, K. I. 2002. New perspectives on the Northern Hemisphere winter storm tracks. *J. Atmos. Sci.,* **59**, 1041-1061. doi: 10.1175/1520-0469(2002)059<1041:NPOTNH>2.0.CO;2.

Hunter, A., Stephenson, D.B., Economou, T., Holland, M. and Cook, I. 2016. New perspectives on the aggregated risk of extratropical cyclones. *Q. J. Roy. Meteorol. Soc.* **142**, 243–256. doi:10.1002/qj.2649.

Huntingford, C., Marsh, T., Scaife, A. A., Kendon, E. J., Hannaford, J. and co-authors 2014. Potential influences in the United Kingdom's floods of winter 2013–2014. *Nat. Clim. Change* **4**, 769–777. doi: 10.1038/nclimate2314.

Hurrell, J. W., Kushnir, Y., Ottersen, G. and Visbeck, M. 2003. An Overview of the North Atlantic Oscillation, in The North Atlantic Oscillation: Climatic Significance and Environmental Impact (eds J. W. Hurrell, Y. Kushnir, G. Ottersen and M. Visbeck), American Geophysical Union, Washington, D. C. doi: 10.1029/134GM01.

Inatsu, M., 2009: The neighbor enclosed area tracking algorithm for extratropical wintertime cyclones. *Atmos. Sci. Lett.* **10**, 267-272. doi: 10.1002/asl.238.

Karremann, M. K., Pinto, J. G., Reyers, M., Klawa, M. 2014. Return periods of losses associated with European windstorm series in a changing climate. *Environ. Res. Lett.* **9**, 124016. doi: 10.1088/1748-9326/9/12/124016.

Kew, S. F., Sprenger, M. and Davies, H. C. 2010. Potential vorticity anomalies of the lowermost stratosphere: A 10-yr winter climatology. *Mon. Weather Rev.* **138**, 1234-1249. doi: 10.1175/2009MWR3193.1.

507 Lionello, P., Dalan, F. and Elvini, E. 2002. Cyclones in the Mediterranean region: The present
508 and the doubled CO2 climate scenarios. *Clim. Res.* **22**, 147-159. doi: 10.3354/cr022147.
509 Lionello, P., Trigo, I. F., Gil, V., Liberato, M. L. R., Nissen, K. M., and co-authors. 2016.
510 Objective Climatology of Cyclones in the Mediterranean Region: a consensus view among
511 methods with different system identification and tracking criteria. *Tellus A,* **68**, 29391. doi:
512 10.3402/tellusa.v68.29391
513 Mailier, P. J., Stephenson, D. B., Ferro, C. A. T., and Hodges, K. I. 2006. Serial clustering of
514 extratropical cyclones. *Mon. Weather Rev.* **134**, 2224-2240. doi: 10.1175/MWR3160.1.
515 Matthews, T., Murpy, C., Wilby, R. L., and Harrigan, S. 2014. Stormiest winter on record for
516 Ireland and UK. *Nat. Clim. Change* **4**, 738–740. doi: 10.1038/nclimate2336.
517 Messori, G., and Caballero, R. 2015. On double Rossby wave breaking in the North Atlantic.
518 *J. Geophys. Res. Atmos.* **120**, 11129–11150. doi: 10.1002/2015JD023854.
519 Murray, R. J. and Simmonds, I. 1991. A numerical scheme for tracking cyclone centres from
520 digital data. Part I: Development and operation of the scheme. *Aust. Meteorol. Mag.* **39**,
521 155-166.
522 Neu, U., Akperov, M. G., Bellenbaum, N., Benestad, R., Blender, R., and co-authors. 2013.
523 IMILAST - a community effort to intercompare extratropical cyclone detection and
524 tracking algorithms: assessing method-related uncertainties. *Bull. Am. Meteorol. Soc.* **94**,
525 529-547. doi: 10.1175/BAMS-D-11-00154.1.
526 Parker, D. J. 1998. Secondary frontal waves in the North Atlantic region: A dynamical
527 perspective of current ideas. *Q. J. Roy. Meteorol. Soc.* **124**, 829–856.
528 doi: 10.1002/qj.49712454709.
529 Pinto, J. G., Spangehl, T., Ulbrich, U. and Speth, P. 2005. Sensitivities of a cyclone detection
530 and tracking algorithm: Individual tracks and climatology. *Meteorol. Z.* **14**, 823-838. doi:
531 10.1127/0941-2948/2005/0068.

532 Pinto, J. G., and Raible C. C. 2012. Past and recent changes in the North Atlantic oscillation.
533 *Wiley Interdisc. Rev. Clim. Change* **3**, 79–90. doi: 10.1002/wcc.150.
534 Pinto, J. G., Bellenbaum, N., Karremann, M. K., and Della-Marta, P. M. 2013. Serial
535 clustering of extratropical cyclones over the North Atlantic and Europe under recent and
536 future climate conditions, *J. Geophys. Res. Atmos.,* **118**, 12476–12485. doi:
537 10.1002/2013JD020564.
538 Pinto, J. G., Gómara, I., Masato, G., Dacre, H. F., Woollings, T., Caballero, R. 2014. Large-
539 scale dynamics associated with clustering of extra-tropical cyclones affecting Western
540 Europe. *J. Geophys. Res. Atmos.,* **119**, 13704–13719. doi: 10.1002/2014JD022305.
541 Raible, C. C., Della-Marta, P., Schwierz, C., Wernli, H., and Blender, R., 2008. Northern
542 Hemisphere extratropical cyclones: A comparison of detection and tracking methods and
543 different reanalyses. *Mon. Weather Rev.* **136**, 880-897. doi: 10.1175/2007MWR2143.1.
544 Rienecker, M. M., Suarez M. J., Gelaro R., Todling, R., Bacmeister J., and Coauthors. 2011.
545 MERRA: NASA's Modern-Era Retrospective Analysis for Research and Applications. *J.*
546 *Clim.* **24**, 3624–3648. doi: 10.1175/JCLI-D-11-00015.1.
547 Rudeva, I., and Gulev, S.K. 2007. Climatology of cyclone size characteristics and their
548 changes during the cyclone life cycle. *Mon. Weather Rev.* **135**, 2568–2587. doi:
549 10.1175/MWR3420.1.
550 Rudeva, I., Gulev, S. K., Simmonds, I., and Tilinina, N. 2014. The sensitivity of
551 characteristics of cyclone activity to identification procedures in tracking algorithms. *Tellus*
552 *A*, **66**, 24961. doi: 10.3402/tellusa.v66.24961.
553 Serreze, M. C. 1995. Climatological aspects of cyclone development and decay in the Arctic.
554 *Atmos.-Ocean* **33**, 1-23. doi: 10.1080/07055900.1995.9649522

555 Simmonds, I., Keay, K. and Lim, E.-P. 2003. Synoptic activity in the seas around Antarctica.
556 *Mon. Weather Rev.* **131**, 272-288. doi: 10.1175/1520-
557 0493(2003)131<0272:SAITSA>2.0.CO;2.
558 Sinclair, M. R., 1994. An objective cyclone climatology for the Southern Hemisphere. *Mon.*
559 *Wea. Rev.* **122**, 2239-2256. doi: 10.1175/1520-0493(1994)122<2239:AOCCFT>2.0.CO;2.
560 Sinclair, M. R. 1997. Objective identification of cyclones and their circulation intensity, and
561 climatology. *Weather Forecast.* **12**, 595-612. doi: 10.1175/1520-
562 0434(1997)012<0595:OIOCAT>2.0.CO;2.
563 Trigo, I. F. 2006. Climatology and interannual variability of storm-tracks in the Euro-Atlantic
564 sector: a comparison between ERA-40 and NCEP/NCAR reanalyses. *Clim. Dyn.* **26**, 127–
565 143. doi: 10.1007/s00382-005-0065-9.
566 Uppala, S. M., Källberg, P. W., Simmons, A. J., Andrae, U., Bechtold, V. D. C., and co-
567 authors. 2005. The ERA-40 re-analysis. *Q. J. Roy. Meteorol. Soc.* **131**, 2961–3012.
568 doi: 10.1256/qj.04.176.
569 Vitolo, R., Stephenson, D. B., Cook, I. M., and Mitchell-Wallace, K. 2009. Serial clustering of
570 intense European storms. *Meteorol. Z.*, **18**, 411-424. doi: 10.1127/0941-2948/2009/0393
571 Wang, X. L., Swail, V. R. and Zwiers, F. W. 2006. Climatology and changes of extratropical
572 cyclone activity: Comparison of ERA-40 with NCEP-NCAR reanalysis for 1958-2001. *J.*
573 *Clim.* **19**, 3145-3166. doi: 10.1175/JCLI3781.1.
574 Wernli, H. and Schwierz, C. 2006. Surface cyclones in the ERA-40 dataset (1958-2001). Part
575 I: Novel identification method and global climatology. *J. Atmos. Sci.* **63**, 2486-2507. doi:
576 10.1175/JAS3766.1.
577 Zolina, O. and Gulev, S. K. 2002. Improving the accuracy of mapping cyclone numbers and
578 frequencies. *Mon. Weather Rev.* **130**, 748-759. doi: 10.1175/1520-
579 0493(2002)130<0748:ITAOMC>2.0.CO;2.

Figures

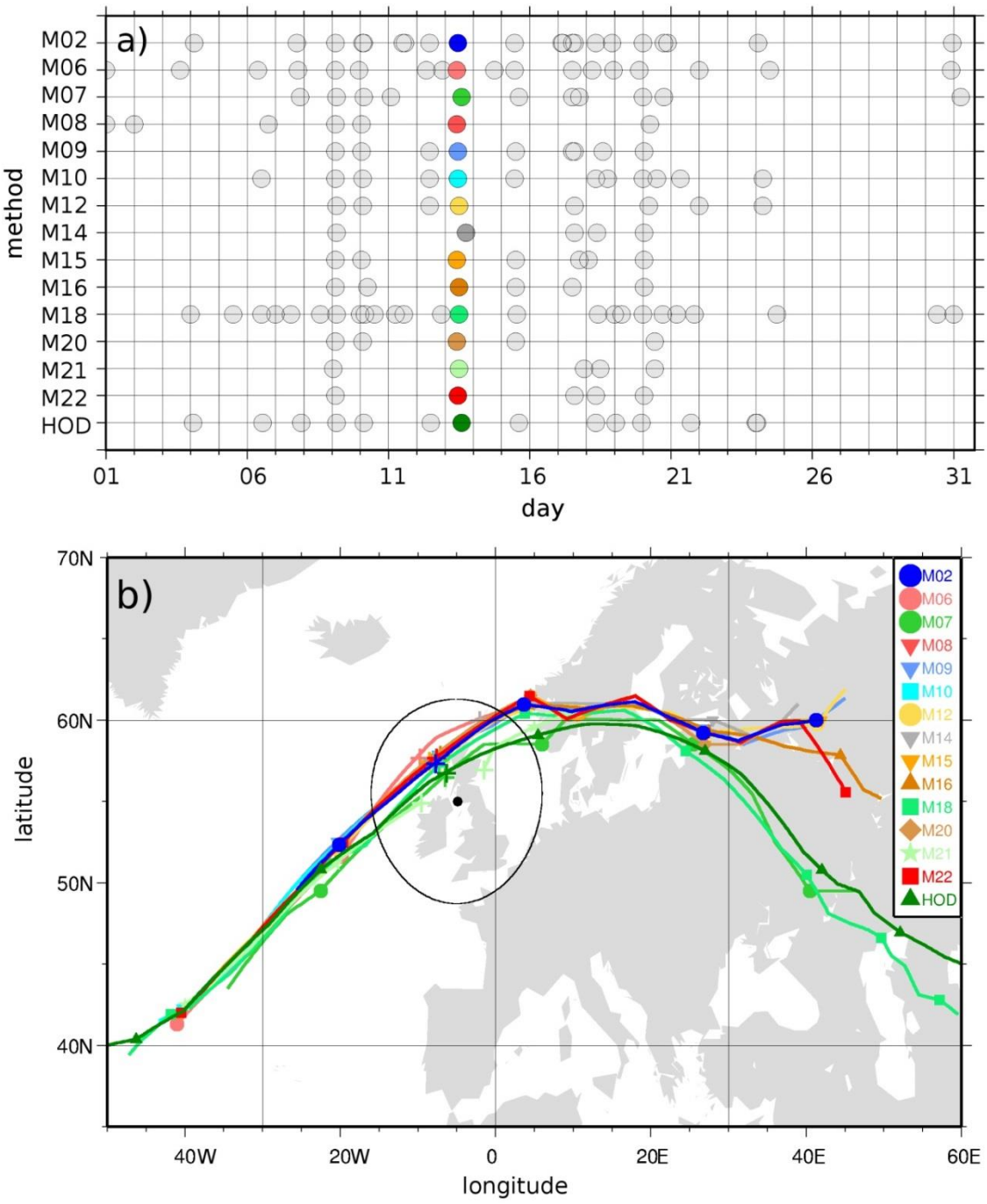

Figure 1: (a) Cyclone count time series of cyclone passages in January 2007 for different methods (M02-M22, cf Table 1) for the grid point 55ºN, 5ºW (black dot in b). Events on January 13th are marked in colour for each method. (b) Map with tracks corresponding to marked events in a). Closest position of the track to the grid point is marked by +.

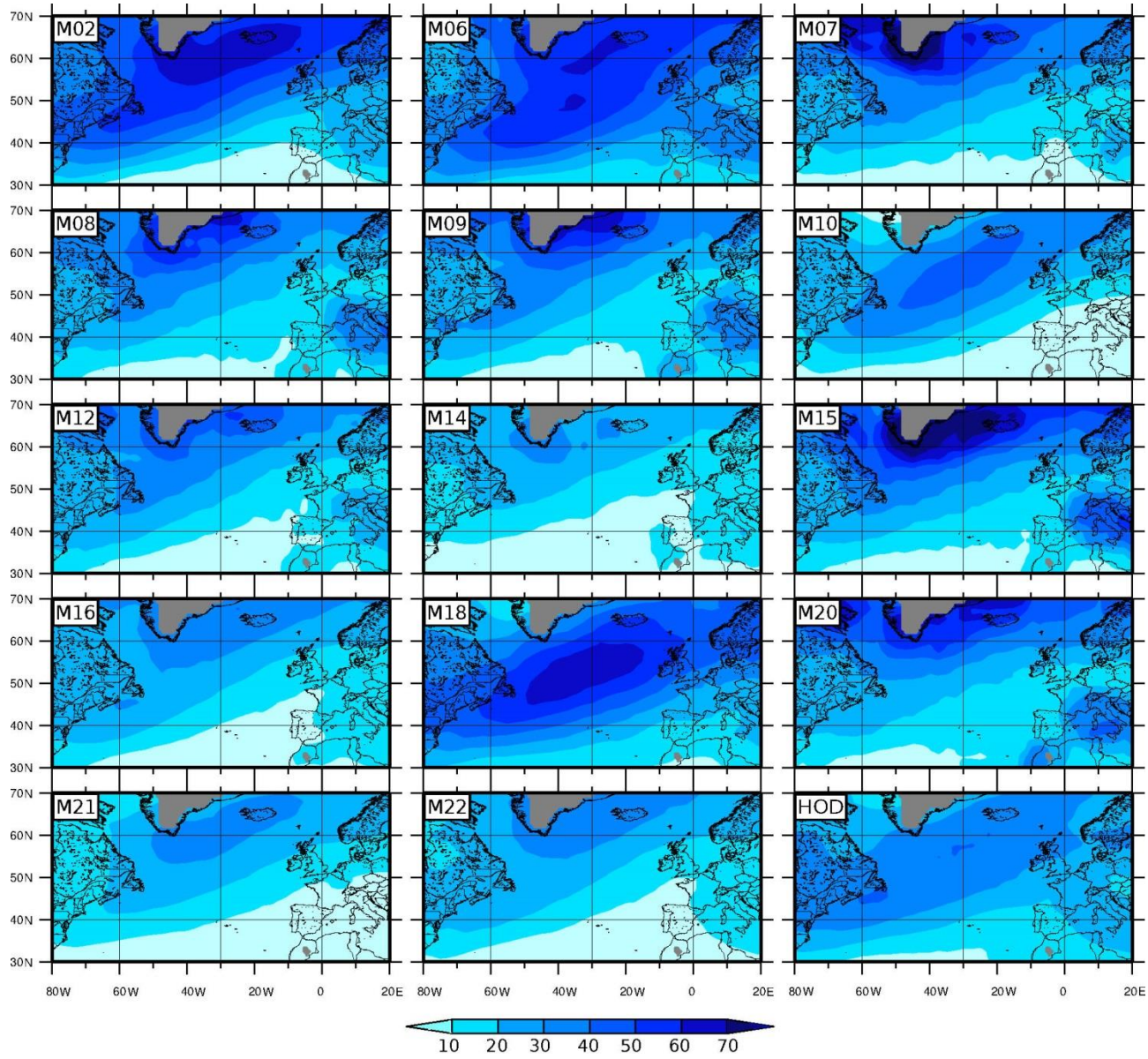

Figure 2: Average number of DJF cyclone passages $\bar{y}$ for each of the 15 methods (M02-M22, HOD) derived from ERA-Interim (1979-2010).

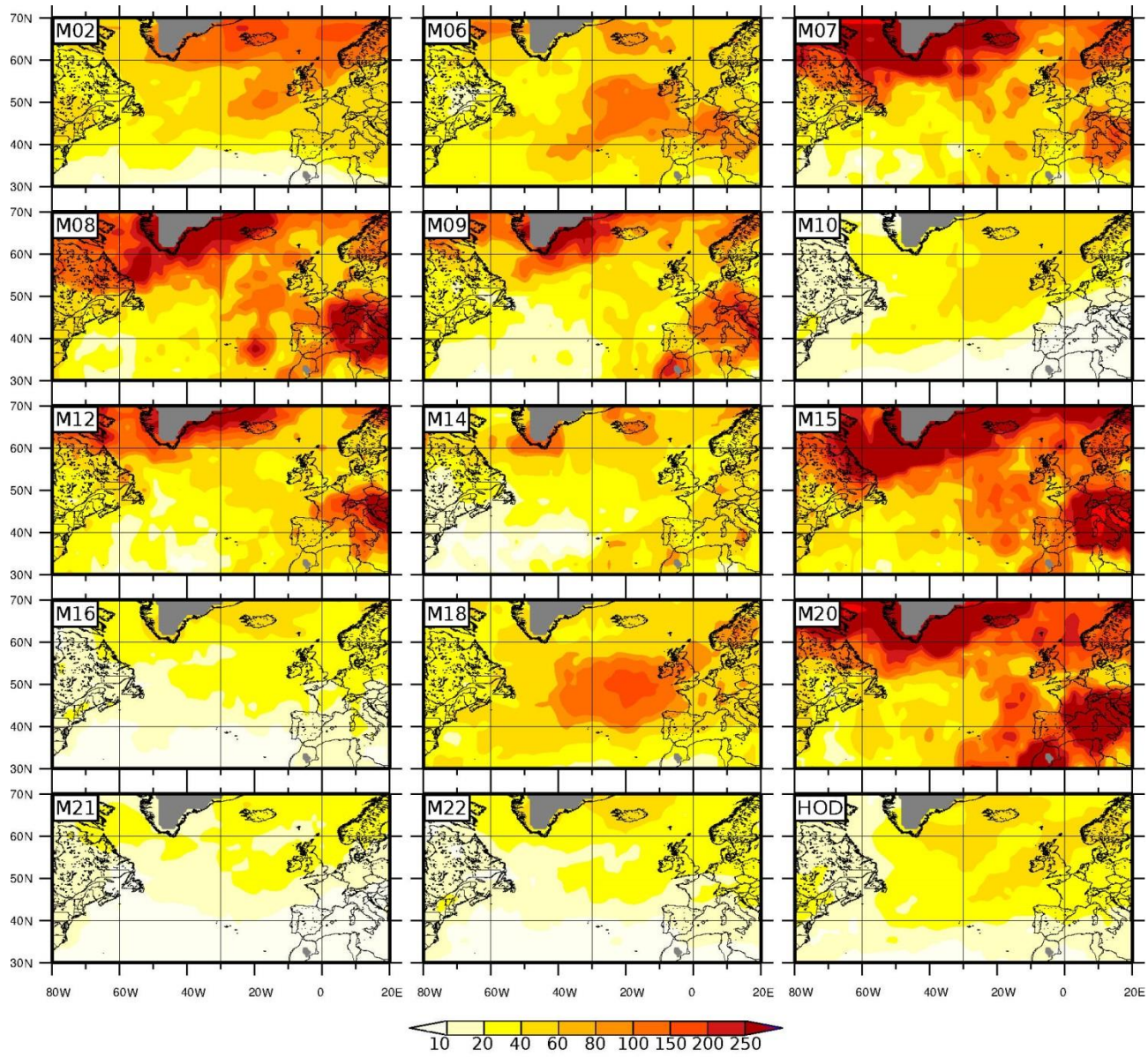

597
598

599 **Figure 3** Variance of DJF cyclone passages $(s_y)^2$ for each of the 15 methods (M02-M22,

600 HOD) derived from ERA-Interim (1979-2010).

601

602
603

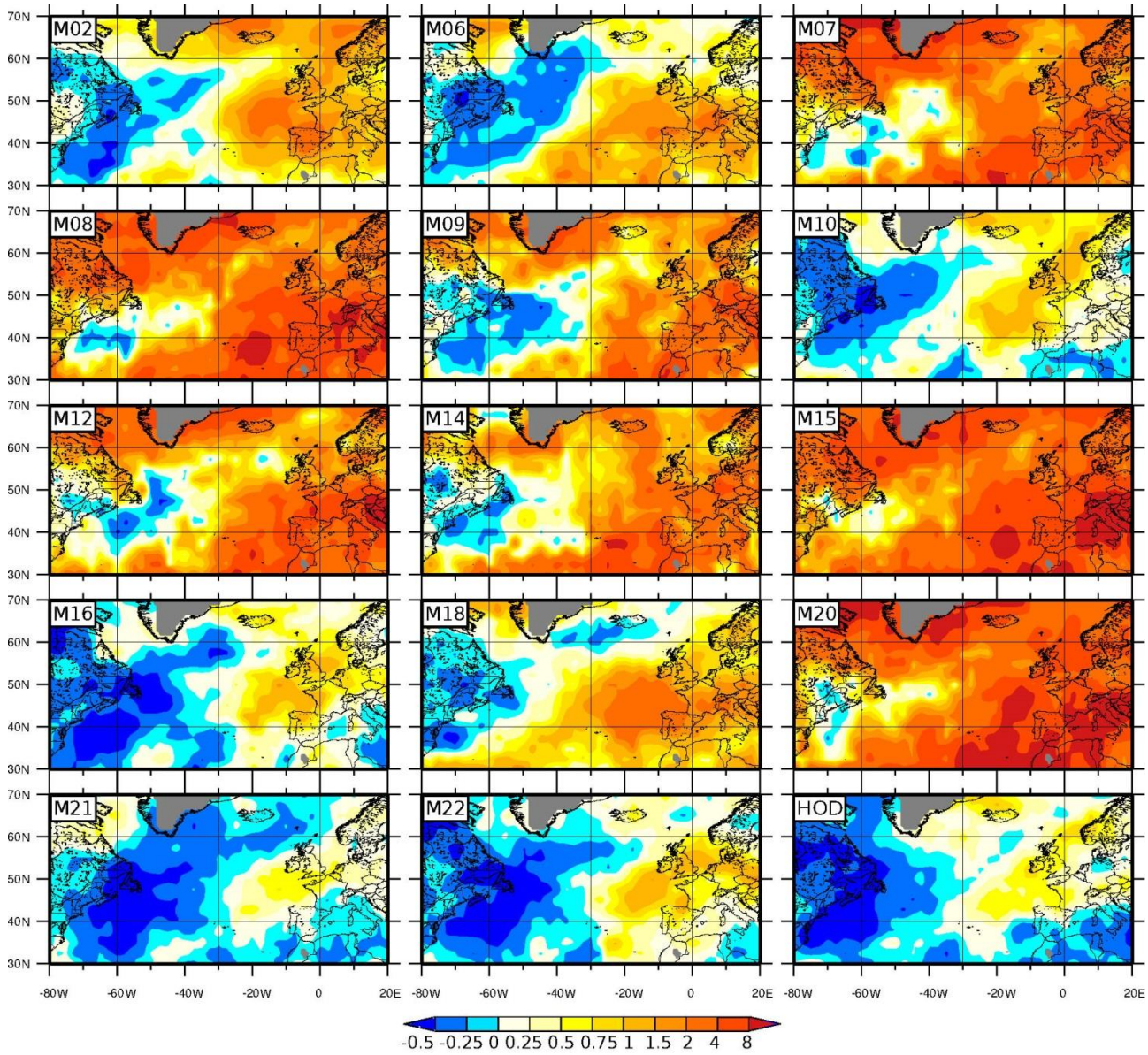

604
605
606 **Figure 4**: Dispersion statistic ϕ for each of the 15 methods (M02-M22, HOD) derived from

607 ERA-Interim (1979-2010).

608
609
610

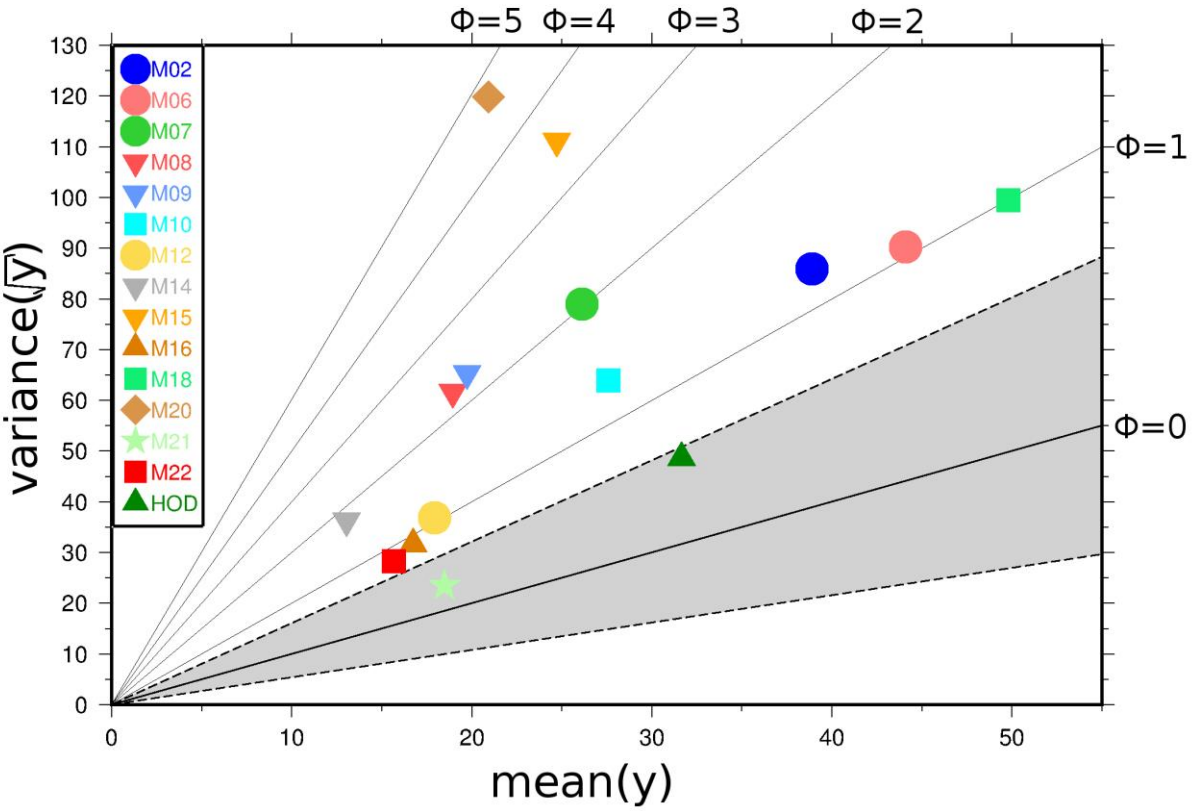

Figure 5: Variance $\left(s_{\sqrt{\bar{y}}}\right)^2$ (y-axis) and mean of cyclone track counts per winter $\bar{y}$ (x-axis) for the grid point 55ºN, 5ºW for each method (M02-M22,HOD). Isolines of dispersion statistic ϕ are depicted in black (for values 0 to 5). The gray area depicts a 95% (bootstrap) confidence interval for the variance, under the assumption of no overdispersion.

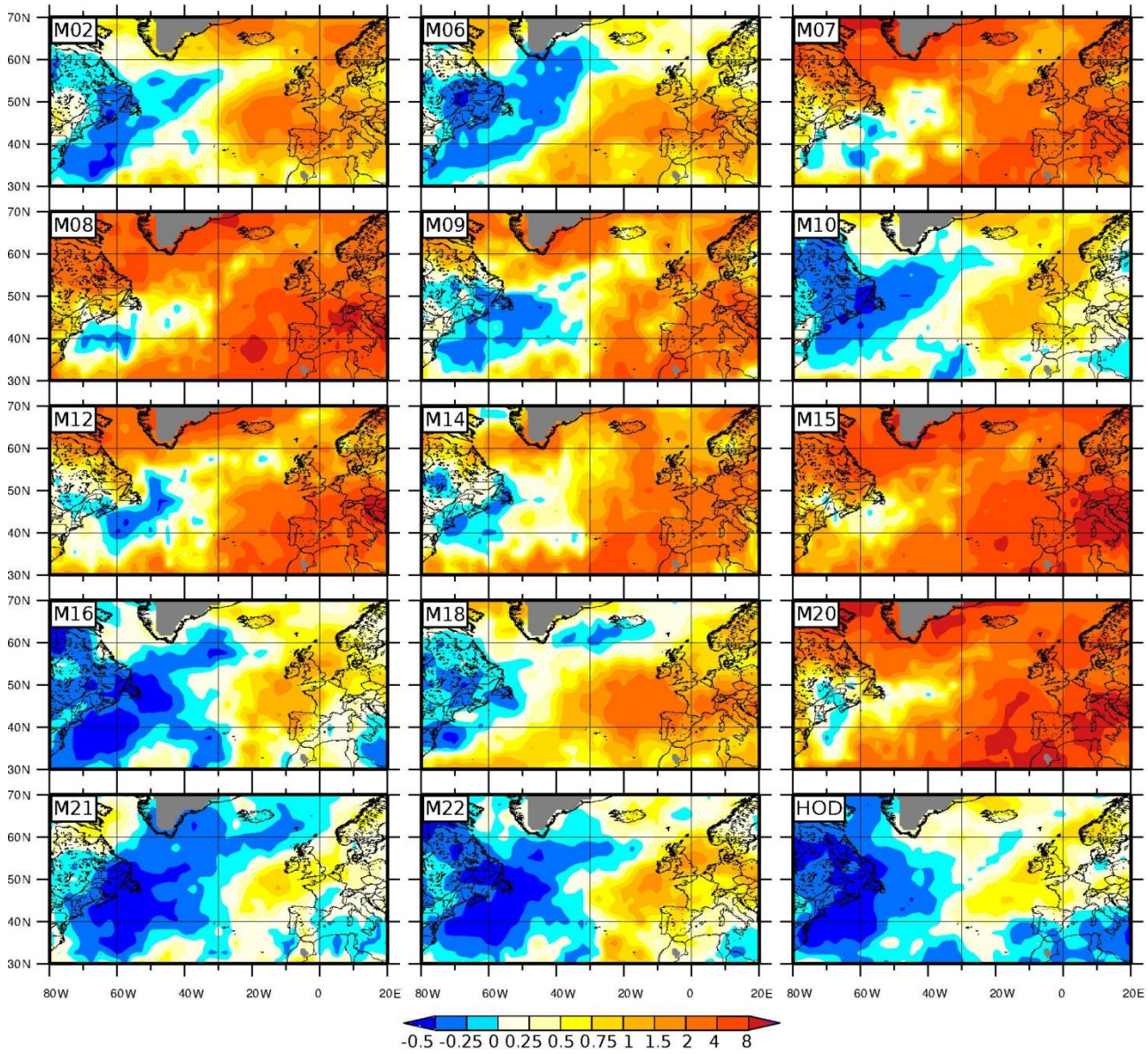

620
621

622 **Figure 6**: Estimated dispersion statistic ϕ' quantified with $4 \cdot \left(s_{\sqrt{y}}\right)^2$-1 for each of the 15

623 methods (M02-M22, HOD) derived from ERA-Interim (1979-2010).

624

625

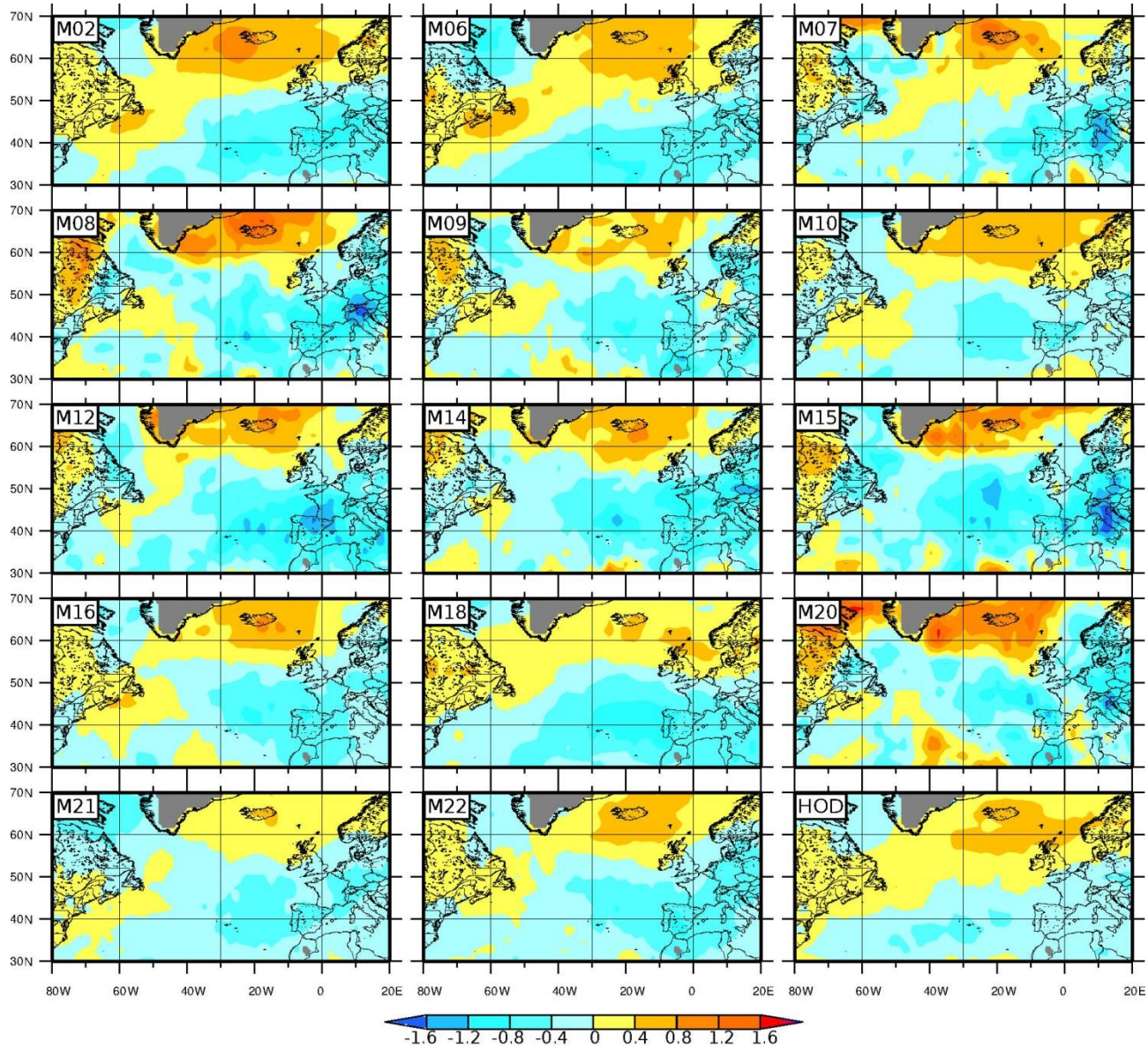

626
627
628 **Figure 7**: Regression coefficient β (see EQ.3) for each of the 15 methods (M02-M22, HOD)

629 derived from ERA-Interim (1979-2010).

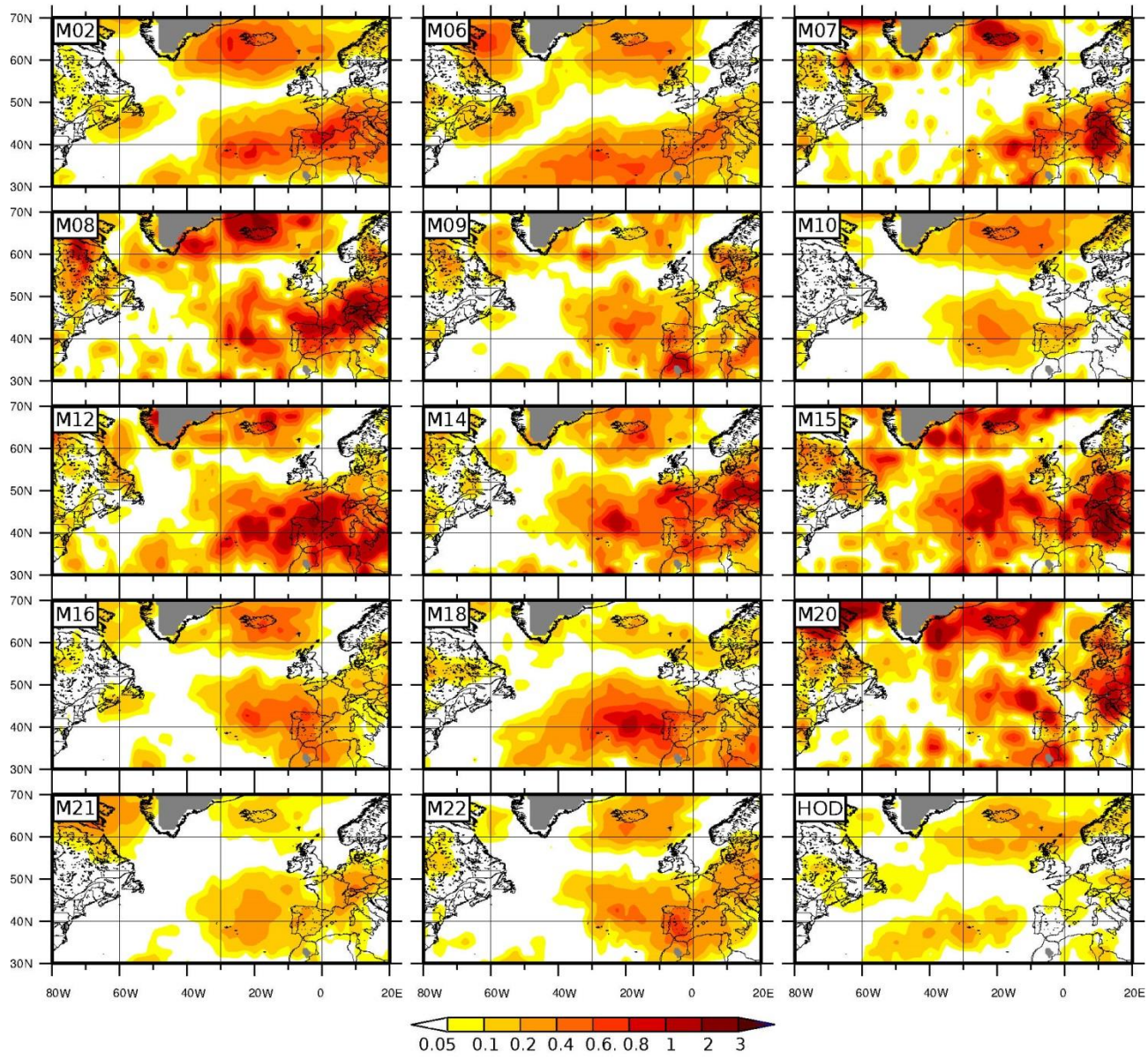

630
631 **Figure 8**: Effect of NAO on dispersion following $4\beta^2(s_x)^2$ for each of the 15 methods (M02-

632 M22, HOD) derived from ERA-Interim (1979-2010).

633

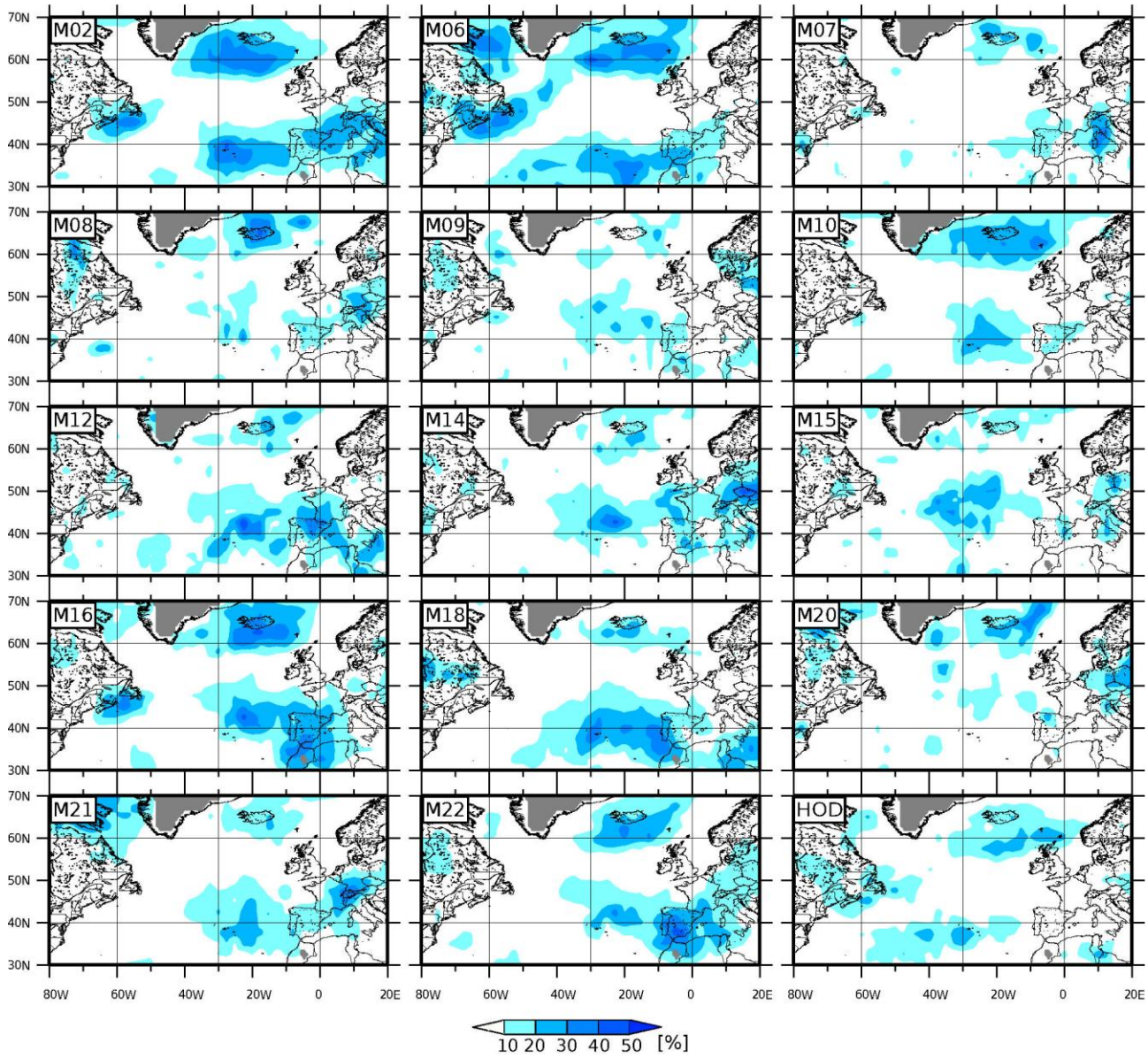

Figure 9: Relative effect of NAO on dispersion following $\beta^2(s_x)^2/\left(s_{\sqrt{y}}\right)^2$ for each of the 15 methods (M02-M22, HOD) derived from ERA-Interim (1979-2010).

640 **Table 1**: List of cyclone tracking methods used in this study according to the IMILAST
641 project denominations (Code M02-M22, HOD), main references of the method description,
642 and main variable used (MSLP: mean sea level pressure; VORT: vorticity or Laplacian of
643 MSLP; Z850 VORT: vorticity at 850 hPa; Z850: geopotential height at 850 hPa; grad.:
644 gradient of MSLP; min: minimum).
645

Code	Main references for method description	Main variable used
M02	Murray and Simmonds (1991), Pinto et al. (2005)	MSLP (min), VORT
M06	Hewson (1997), Hewson and Titley (2010)	MSLP (min. grad.)
M07	Flaounas et al. (2014)	Z850 VORT
M08	Trigo (2006)	MSLP (min. grad.)
M09	Serreze (1995), Wang et al. (2006)	MSLP (min. grad.), VORT
M10	Murray and Simmonds (1991), Simmonds et al. (2003)	MSLP (min), VORT
M12	Zolina and Gulev (2002), Rudeva and Gulev (2007)	MSLP (min)
M14	Kew et al. (2010)	Z850 (min. contour)
M15	Blender et al. (1997), Raible et al. (2008)	MSLP (min)
M16	Lionello et al. (2002)	MSLP (min)
M18	Sinclair (1994, 1997)	Z850 VORT
M20	Wernli and Schwierz (2006)	MSLP (min)
M21	Inatsu (2009)	Z850 VORT
M22	Bardin and Polonsky (2005), Akperov et al. (2007)	MSLP (min. contour)
HOD	Hodges (1994), Hodges (1999), Hodges et al. (2011)	Z850 VORT

646
647

Supplementary Material

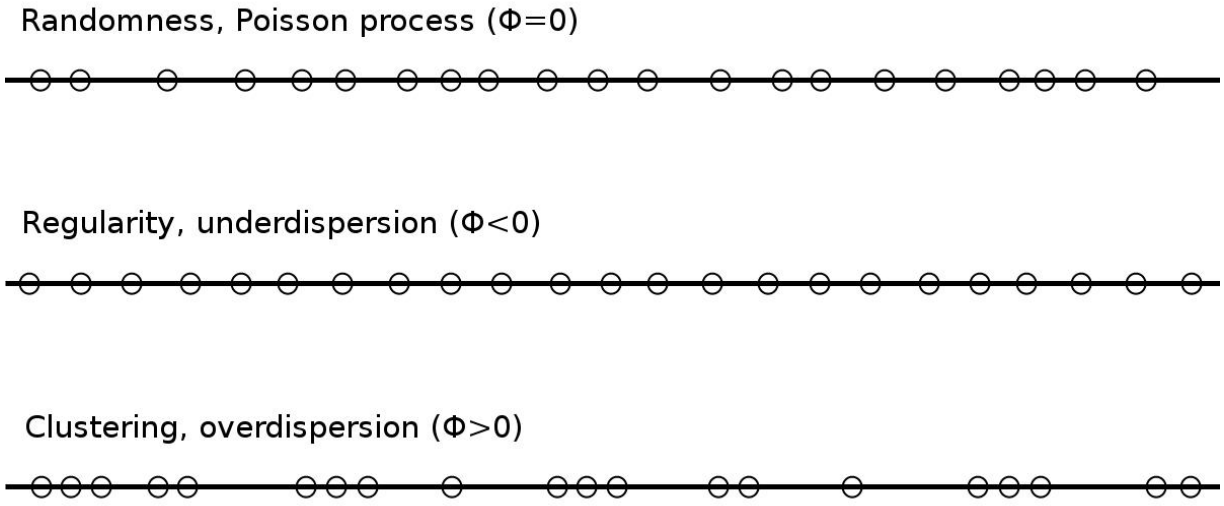

Figure S1: Examples of time series with randomness, regularity and clustering of counts. For more details see text.

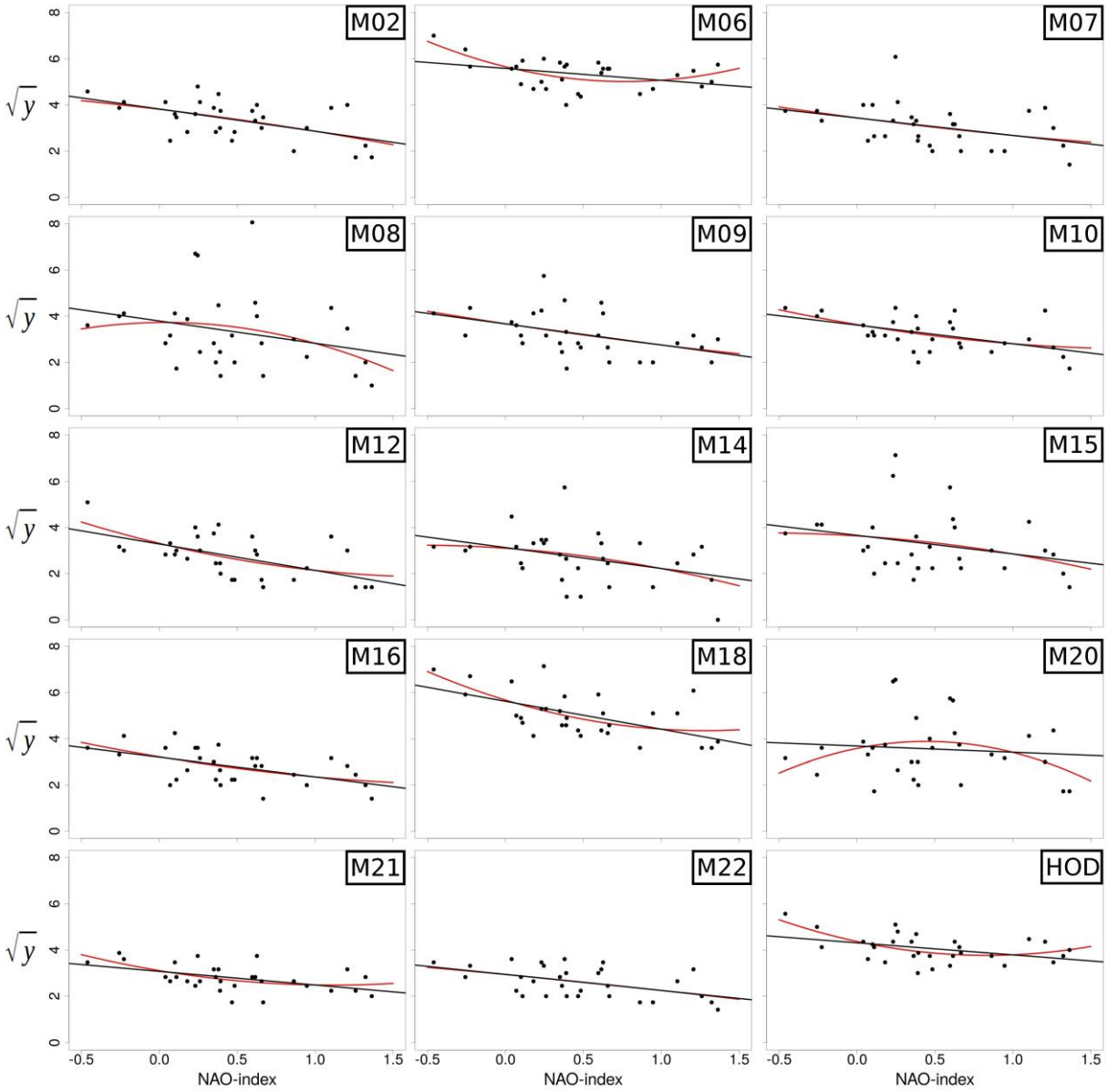

Figure S2: Scatter plot of NAO index and $\sqrt{y}$ of the grid point 40ºN, 20ºW for each of the 15 methods (M02-M22, HOD) derived from ERA-Interim (1979-2010) including the linear (black line) and the quadratic (red line) fits.

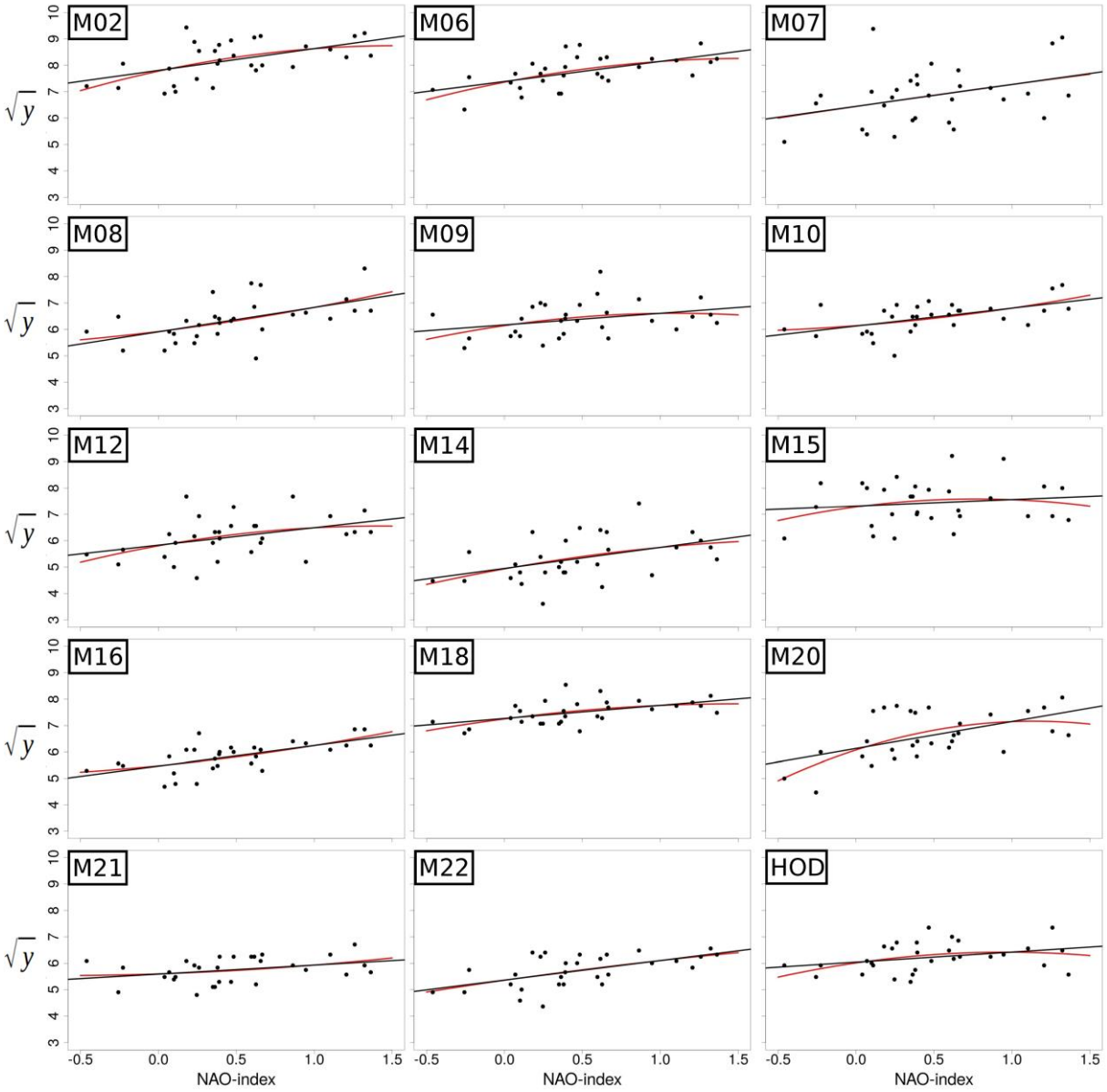

662
663

664 **Figure S3**: Scatter plot of NAO index and $\sqrt{y}$ of the grid point 62.5ºN, 20ºW for each of the

665 15 methods (M02-M22, HOD) derived from ERA-Interim (1979-2010) including the linear

666 (black line) and the quadratic (red line) fits.

667
668